Cell Death & Differentiation (2020) 27:2843–2855
https://doi.org/10.1038/s41418-020-0546-8

Cell Death & Differentiation

ARTICLE

Critical role of histone H3 lysine 27 demethylase Kdm6b in the homeostasis and function of medullary thymic epithelial cells

Zhi Liu[1,2,5] · Haohao Zhang[1,2] · Yiming Hu[1,2] · Dandan Liu[2] · Lingling Li[2] · Cuifeng Li[1,2] · Qi Wang[2] · Junhaohui Huo[2] · Hanshao Liu[1,2] · Ningxia Xie[1,2] · Xingxu Huang[1] · Yongzhong Liu[3] · Charlie Degui Chen[4] · Yufang Shi[2] · Xiaoren Zhang[1,2]

Received: 26 October 2019 / Revised: 3 April 2020 / Accepted: 7 April 2020 / Published online: 28 April 2020

Abstract

Medullary thymic epithelial cells (mTECs) play a central role in the establishment of T cell central immunological tolerance by promiscuously expressing tissue-restricted antigens (TRAs) and presenting them to developing T cells, leading to deletion of T cells responding to self-antigens. However, molecular mechanisms especially epigenetic regulation of mTEC homeostasis and TRA expression remain elusive. Here we show that the H3K27 demethylase Kdm6b is essential to maintain the postnatal thymic medulla by promoting mTEC survival and regulating the expression of TRA genes. Moreover, mice lacking Kdm6b developed pathological autoimmune disorders. Mechanically, Kdm6b exerted its function by reducing repressive H3K27 trimethylation (H3K27me3) at the promoters of anti-apoptotic gene *Bcl2* and a set of Aire-dependent TRA genes. Thus, our findings reveal a dual role of Kdm6b in the regulation of mTEC-mediated T cell central tolerance.

Introduction

The unique capability of the thymus is to 'educate' immature T lymphocytes to become mature cells both major histocompatibility complex (MHC)-restricted and nonself-reactive [1]. TECs are essential for this educational process as they control the development and selection of T lymphocytes to functionally competent T cells [2]. Based on their anatomical localization, phenotype and function, TECs are mainly divided to two distinct subpopulations. Cortical (c)TECs are critical for positive selection of developing T cells, whereas mTECs have a primary role in the negative selection of autoreactive T cells and generation of thymic T regulatory (Treg) cells [3, 4]. This fundamental role of mTECs is attributed to their unique ability to promiscuously express tissue-restricted antigens (TRAs) and present TRAs to developing T cells [5, 6]. The expression of TRAs is mainly regulated by the autoimmune regulator Aire and transcription factor Fezf2 [7, 8]. Mutations in Aire cause autoimmune polyendocrinopathy candidiasis ectodermal dystrophy (APECED) in humans with developing autoantibodies and immune infiltrates against multiple periphery tissues [9].

TEC differentiation involves a stepwise process. A common bi-potent thymic epithelial progenitor gives rise to cTEC and mTECs lineages [10]. While the developmental cues governing cTEC lineage remain elusive, the mTEC

These authors contributed equally: Zhi Liu, Haohao Zhang, Yiming Hu

Edited by D.R. Green

Supplementary information The online version of this article (https://doi.org/10.1038/s41418-020-0546-8) contains supplementary material, which is available to authorized users.

✉ Xiaoren Zhang
xrzhang@sibs.ac.cn

[1] Affiliated Cancer Hospital and Institute of Guangzhou Medical University, Guangzhou Municipal and Guangdong Provincial Key Laboratory of Protein Modification and Degradation, State Key Laboratory of Respiratory Disease, Guangzhou 510000, China

[2] CAS Key Laboratory of Tissue Microenvironment and Tumor, Shanghai Institute of Nutrition and Health, Shanghai Institutes for Biological Sciences, University of Chinese Academy of Sciences, Chinese Academy of Sciences, Shanghai 200031, China

[3] State Key Laboratory of Oncogenes and Related Genes, Shanghai Cancer Institute, Renji Hospital, Shanghai Jiao Tong University School of Medicine, Shanghai 200032, China

[4] State Key Laboratory of Molecular Biology, Institute of Biochemistry and Cell Biology, Shanghai Institutes for Biological Sciences, Chinese Academy of Sciences, Shanghai 200031, China

[5] Present address: Nomis Foundation Laboratories for Immunobiology and Microbial Pathogenesis, The Salk Institute for Biological Studies, La Jolla, CA 92037, USA

developmental program primarily dependent on the non-canonical NF-κB pathway, activated by several members of TNF receptor family, including RNAK, CD40 and LTβR [11–13]. Indeed, disruption of these receptors and downstream signaling components, such as TRAF6, RelB, NF-κB2, Bcl-3, results in the defects of mTECs and the development of autoimmunity [14–17]. Along with the maturation of mTECs, the expression of MHCII, co-stimulatory molecules CD80 and CD86, Aire and TRAs was gradually increased [18].

In addition to transcription factors, epigenetic modifications such as DNA methylation and histone modification play indispensable roles in cell differentiation and function [19]. Although previous studies have begun to reveal how Aire recognizes the repressive chromatin state of Aire-dependent TRA genes and regulate their expression through cooperation with its partners [20–24], epigenetic regulations of mTEC development and function are yet to be explored. Kdm6b is a histone H3K27 demethylase, catalyzing the conversion of H3K27me3 to H3K27me1 [25]. In the immune system, Kdm6b is critical for M2 macrophage differentiation, T cell development in the thymus and NKT development [26–28]. We and others previously found that Kdm6b is critical for Th17 cell differentiation [29, 30]. Here, we provide another layer of evidence for a pivotal role of Kdm6b in the establishment of T cell central tolerance by regulating mTEC survival, Aire-dependent TRA expression and mTEC function.

Results

Kdm6b is not essential for TEC development in embryos

Kdm6b$^{-/-}$ mice died perinatally due to premature development of lung tissues [31], but its role in other tissues has not been defined. To this end, we performed a tissue survey of Kdm6b expression on mouse tissues by real-time quantitative PCR (RT-qPCR). We found that *Kdm6b* was most highly expressed in the thymus, followed by the spleen and lung (Fig. S1A). Furthermore, the mRNA level of *Kdm6b* was increased gradually during thymus organogenesis and reached its peak at the age of 4 weeks (Fig. S1B). To better assess its expression among different cell types in the thymus, we quantified its mRNA level in FACS-sorted CD45^{+} thymocytes, TECs, cTECs and mTECs, and found that *Kdm6b* was increased postnatally and maintained at a high level in all the populations from day 7 (Fig. 1a, b), indicating a broad effect of Kdm6b on thymus development. Indeed, Kdm6b has been shown to be crucial for thymocyte differentiation [27]. Here, we mainly focus on its role in the thymic epithelium.

We initially characterized the function of Kdm6b in constitutive *Kdm6b*$^{-/-}$ thymus at embryonic day 18 (E18). Kdm6b deletion did not affect the development of K8^{+} cTECs, K5^{+} mTECs and ERTR7^{+} thymic fibroblasts. Moreover, the MTS10^{+} mTECs, UEA^{+} and Aire^{+} mature

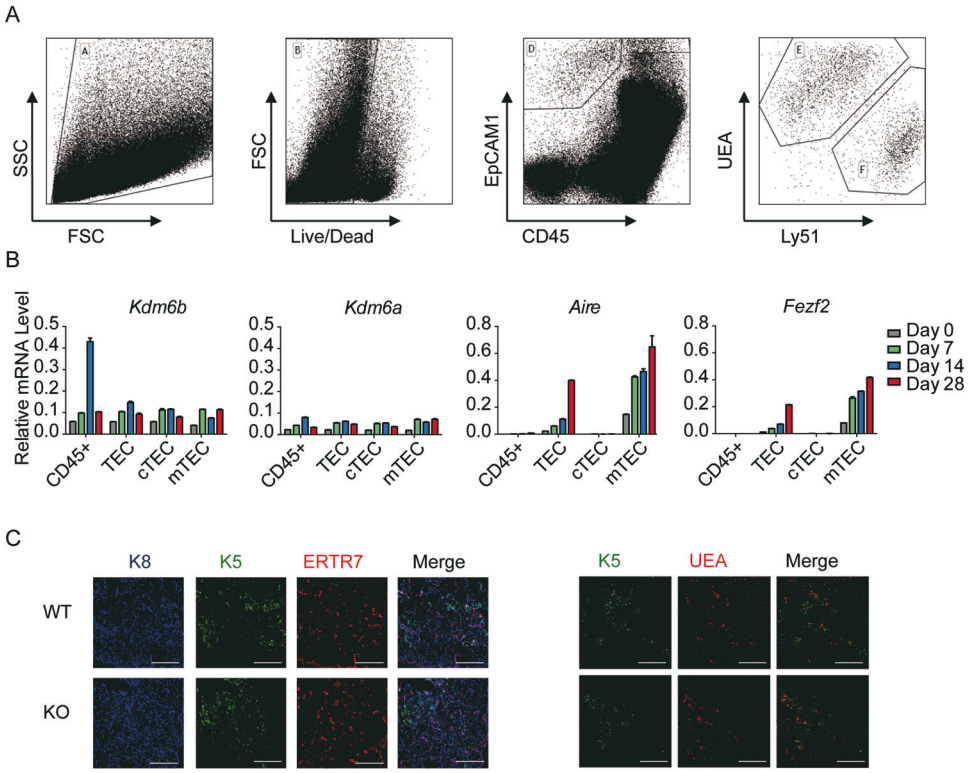

Fig. 1 Kdm6b is not essential for TEC development in embryos. a Strategy of sorting thymocytes and thymic epithelial cell populations. **b** Expression of *Kdm6b*, *Kdm6a*, *Aire* and *Fezf2* in FACS-sorted thymocytes, TECs, cTECs and mTECs at different time points analyzed by RT-qPCR ($n = 3$). **c** Immunofluorescent staining of thymus sections from indicated mice at the age of E18 with Keratin-8(K8), a cTEC marker; Keratin-5(K5), a mTEC marker; ERTR7, a fibroblast maker; UEA-1, a mature mTEC marker. Scale bars, 75 μm ($n = 4$ per genotype).

mTECs were all comparable between *Kdm6b*$^{-/-}$ mice and wild-type controls (Fig. 1c and S2A). Besides, the mRNA levels of cTEC associated gene *CstL*, mTEC associated genes (*RANK*, *Cd80*, *MHCII* and *Aire*), and some of TRA genes (*Ins2*, *Crp*, *Csna* and *Cnsb*) were not different between *Kdm6b*$^{-/-}$ and controls (Fig. S2B). Therefore, Kdm6b deletion has little impact on TEC development in embryos.

Kdm6b maintains the postnatal homeostasis of mTECs

To fully assess the role of Kdm6b in the postnatal development of TECs, we further generated mice carrying floxed exons 14–20 of *Kdm6b* alleles (*Kdm6b*$^{fl/fl}$) [32] and crossed them with mice expressing the Cre recombinase driven by thymic-epithelial specific *Foxn1* locus (*Foxn1*-Cre). We observed complete deletion of the target allele in TECs isolated from the resultant homozygous mice (called '*Kdm6b*$^{fl/fl}$*Foxn1*-Cre mice') as early as E14 (Fig. S2C, D).

We first analyzed the thymus of *Kdm6b*$^{fl/fl}$*Foxn1*-Cre mice at the age of 4 weeks when the cellularity of CD45$^-$ cells reach their peak [33]. The area of medullary compartment of mutant mice was strikingly smaller when compared to wild-type controls, while the segregation from the cortex was maintained (Fig. 2a). To gain more in-depth information, we employed flow cytometry to precisely characterize the impairment of TECs in *Kdm6b*$^{fl/fl}$*Foxn1*-Cre mice. The frequency and absolute number of mTECs (CD45$^-$EpCAM$^+$Ly51$^-$UEA$^+$) were dramatically reduced in *Kdm6b*$^{fl/fl}$*Foxn1*-Cre mice, whereas the absolute number of cTECs (CD45$^-$EpCAM$^+$Ly51$^+$UEA$^-$) was comparable to wild-type controls (Fig. 2b). mTECs are a heterogeneous population composed of immature MHCII^{lo}CD80^{lo} and mature MHCII^{hi}CD80^{hi} mTEC subsets, with the latter one containing a fraction expressing Aire [34]. The percentage of Aire$^+$ mTECs was maintained normally in the whole mTEC population (CD45$^-$EpCAM$^+$UEA$^+$) of *Kdm6b*$^{fl/fl}$ *Foxn1*-Cre mice (Fig. 2c), as indicated by the similar ratio of Aire$^+$ to Aire$^-$ mTECs when compared to wide-type controls (Fig. 2c). However, due to the overall loss of mTEC cellularity, the absolute number of Aire$^+$ and Aire$^-$ mTECs were both reduced significantly in Kdm6b-deficient thymus (Fig. 2c). Similarly, the ratio of MHCII^{hi}CD80^{hi} to MHCII^{low}CD80^{low} mTECs in the whole mTEC population was similar between *Kdm6b*$^{fl/fl}$*Foxn1*-Cre mice and wide-type controls (Fig. 2d), while the absolute number of MHCII^{hi}CD80^{hi} and MHCII^{low}CD80^{low} mTECs were reduced proportionally in Kdm6b-deficient thymus (Fig. 2d). These data suggest that Kdm6b specifically controls the cellularity of medullary compartment.

To fully determine when the cellularity of mTECs start to lose, we next monitored the changes of TECs in the first two weeks of life. Consistent with constitutive *Kdm6b*$^{-/-}$ mice, the percentage and absolute number of cTECs and mTECs in *Kdm6b*$^{fl/fl}$*Foxn1*-Cre mice was identical to wide-type controls at PN0. However, the percentage and absolute number of mTECs was significantly decreased at PN7 and thereafter in *Kdm6b*$^{fl/fl}$*Foxn1*-Cre mice (Fig. 2e). Furthermore, immunofluorescence staining confirmed the above observations. The entire K5$^+$ medulla area was dramatically smaller in *Kdm6b*$^{fl/fl}$*Foxn1*-Cre mice than wild-type controls at the age of 4 and 8 weeks, but comparable at PN0 (Fig. 2f). Consistently, the UEA$^+$ and Aire$^+$ mTECs were significantly reduced in the whole thymus of *Kdm6b*$^{fl/fl}$ *Foxn1*-Cre mice but maintained normally in the medullary compartment (Fig. S3A). Next, we used RT-qPCR to analyze gene expression in FACS-sorted whole TECs (CD45$^-$ EpCAM$^+$) at the age of 4 weeks. In contrast to gene expression of E18 *Kdm6b*$^{-/-}$ TECs (Fig. S2A), the mRNA levels of cTEC associated genes, including *CstL*, *Psmb11*, *Dll4*, *Il7*, *Cxcl12* and *Ccl25*, were increased significantly, while mTEC associated genes, such as *CtsS*, *RANK*, *Cd80*, *MHCII*, *Aire*, *Fezf2*, and several TRAs including *Ins2* (Aire-dependent), *CRP* (Aire-independent) and *Ttr* (Fezf2-dependent), were dramatically reduced in *Kdm6b*$^{fl/fl}$ *Foxn1*-Cre thymus when compared to wild-type controls (Fig. S3B). Altogether, these data demonstrate that Kdm6b is essential for the postnatal maintenance of mTEC homeostasis, but not for the maturation of mTEC^{low} to mTEC^{hi}.

Defective generation of thymic Treg cells in *Kdm6b*$^{fl/fl}$*Foxn1*-Cre mice

Thymic medulla provides a unique niche for the selection and maturation of conventional T cells and regulatory T cells [35]. We subsequently examined whether loss of mTECs together with reduced expression of TRAs in *Kdm6b*$^{fl/fl}$*Foxn1*-Cre mice impairs mTEC-mediated T cell development. Flow cytometry analysis showed that the differentiation of thymocytes into CD4$^-$CD8$^-$ double negative (DN1 to DN4), CD4$^+$CD8$^+$ double positive (DP) and CD4$^+$/CD8$^+$ single positive (SP) T cells was normal in the thymus of *Kdm6b*$^{fl/fl}$*Foxn1*-Cre mice (Fig. 3a), suggesting that positive selection of developing T cells was intact in the mutant mice. Furthermore, the distribution of CD4$^+$ and CD8$^+$ T cells was normal in the spleen. We did not observe any increased percentage of activated/memory CD44^{hi}CD62L^{low} T cells in the spleens of mutant mice at the age of 4 weeks (Fig. 3d). However, the frequency of Treg cells was significantly reduced in the thymus of 4-week-old mutant mice (Fig. 3b, c), but was identical in the spleen (Fig. 3c–e), which suggested that mTECs did not function properly to support thymic Treg cell differentiation in *Kdm6b*$^{fl/fl}$*Foxn1*-Cre mice.

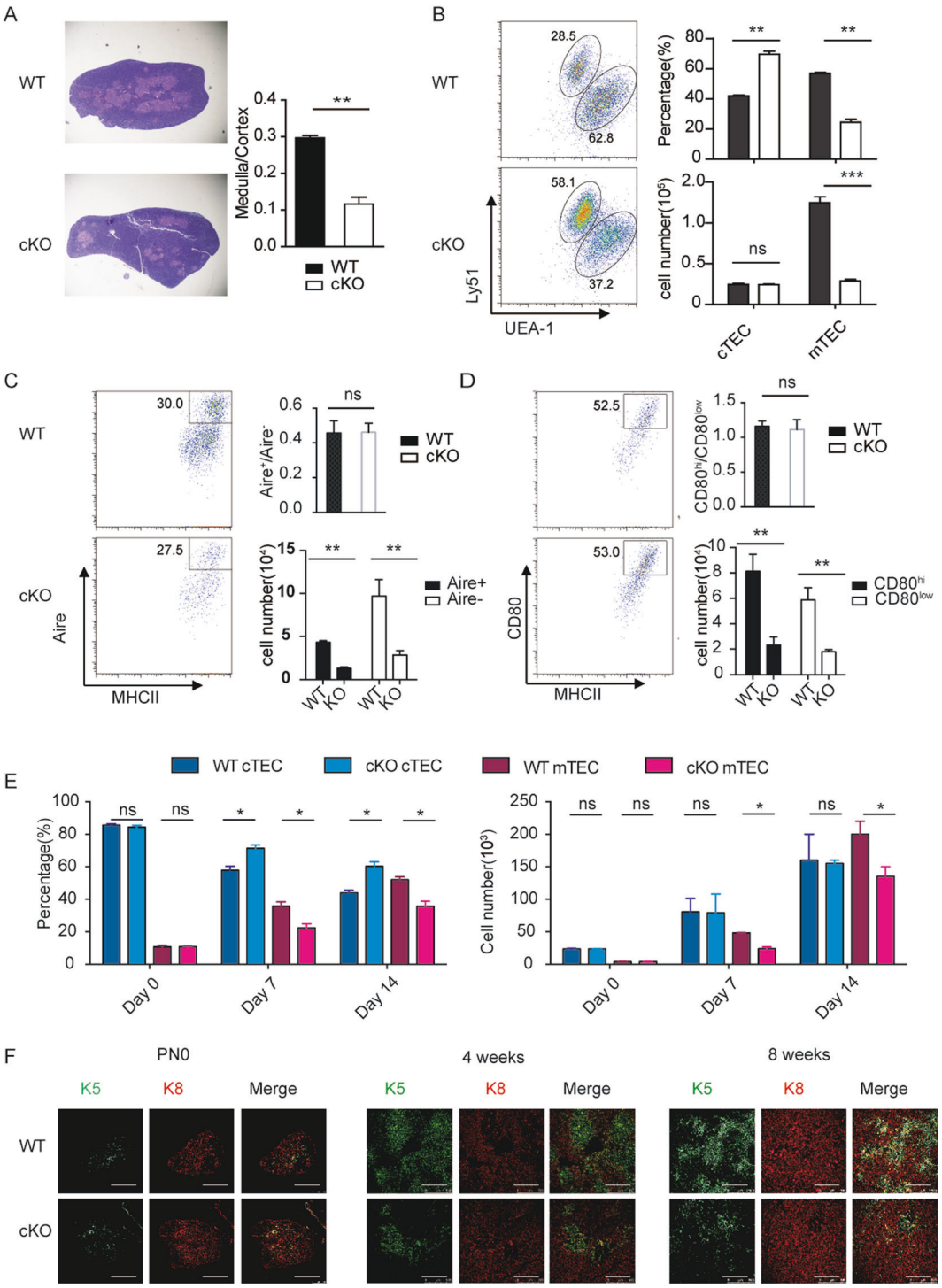

Loss of Kdm6b leads to autoimmune disorders

The massive decrease of mTECs, compromised expression of TRAs and reduced number of thymic Treg cells in *Kdm6b*$^{fl/fl}$*Foxn1*-Cre mice lead us to speculate that Kdm6b deficiency might elicit a failure of self-tolerance and organ-specific autoimmunity. At first, we did not observe lymphocyte infiltrates in the organs such as the liver, pancreas and salivary glands (C57BL/6 background) up to six months. Genetic backgrounds of mouse strain strongly influence the severity of autoimmunity, as demonstrated by Diane Mathis and Christophe Benoist group that even for Aire knockout mice, the autoimmune disorders are "particularly strong on the NOD background, but very mild on the C57BL/6 background" [36]. We reason that the autoimmune phenotype could be likely to observe on BALB/c

◀ **Fig. 2 Kdm6b deficiency reduces the size of medullary compartment and the number of mTECs. a** Representative images of hematoxylin and eosin (H&E) staining of the thymus and morphometric analysis of cortical and medullary areas represented as a ratio (20 sections per thymus of 3 pairs of *Kdm6b*$^{fl/fl}$*Foxn1*-Cre mice and wild-type controls). **b** Flow cytometric profiles of thymic epithelial cells (CD45$^-$EpCAM$^+$) from 4-week-old wild-type and *Kdm6b*$^{fl/fl}$*Foxn1*-Cre mice for the cell surface Ly51 and UEA-1 lectin (left). Frequency and absolute number of cTECs (Ly51$^+$UEA-1$^-$) and mTECs (Ly51$^-$UEA-1$^+$) are shown (right) ($n = 10$ per genotype). **c** Flow cytometric profiles of Aire-expressing mTECs in the whole mTECs (CD45$^-$EpCAM$^+$Ly51$^-$UEA$^+$) from 4-week-old wild-type and *Kdm6b*$^{fl/fl}$*Foxn1*-Cre mice. The ratio of Aire$^+$ mTECs to Aire$^-$ mTECs, as well as the absolute numbers of them are shown in the graphs on the right ($n = 6$ per genotype). **d** Flow cytometric profiles of mTECs from 4-week-old mice for the expression of cell surface MHCII and CD80(left). The ratio of CD80^{hi} mTECs to CD80^{low} mTECs, as well as the absolute numbers of them, are shown in the graphs on the right ($n = 6$ per genotype). **e** The percentage and absolute numbers of mTECs and cTECs in wild-type and *Kdm6b*$^{fl/fl}$*Foxn1*-Cre mice during the first two weeks ($n = 3$ per genotype). **f** Immunofluorescent staining of thymus sections from indicated mice at the age of postnatal day 0 (PN0), 4 weeks and 8 weeks with Keratin-5(K5), UEA-1 and Keratin-8 (K8). Scale bars, 500 μm ($n = 4$ per genotype).

background. Therefore, we next did a thymic transplantation experiment by isolation of fetal thymi from E14.5 *Kdm6b*$^{-/-}$ and control embryos, depletion of thymocyte with 2'-deoxyguanosine (2-dG) for 4 days, and grafting them under the renal capsule of BAB/c nude mice. 10 weeks after grafting, the generation of thymocytes and distribution of T cells in the spleen were normal in recipients grafted with *Kdm6b*$^{-/-}$ thymi (knock-out/nude, KO/nu) mice and in recipients grafted with control thymi (wild-type/nude, WT/nu) (Fig. 4a). However, histological staining showed that 6 out of 10 KO/nu mice had inflammatory infiltrates in the salivary gland, pancreas and liver, while none of 12 WT/nu mice had any lymphocyte infiltrates in the tissues analyzed (Fig. 4b, c). Therefore, Kdm6b plays an indispensable role in preventing autoimmunity.

Increased apoptosis of mTECs in *Kdm6b*$^{fl/fl}$*Foxn1*-Cre mice

Kdm6b plays different roles in the regulation of cell proliferation and/or apoptosis in different cell types [37, 38]. To understand the reason why Kdm6b deficiency leads to loss of mTECs, we next examined spontaneous programmed cell death and cell proliferation in primary mTECs. The percentage of cells positive for cleaved caspase-3, a marker of apoptosis, was significantly increased in mTECs, but not in cTECs, of 4-week-old *Kdm6b*$^{fl/fl}$*Foxn1*-Cre mice when compared to wild-type controls (Fig. 5a). In contrast, the percentage of Ki67$^+$ proliferating mTECs, as well as cTECs, was only slightly reduced in 4-week-old mutant mice in comparison to controls (Fig. S4A, B). Moreover, this was supported by analysis of BrdU incorporation with a single dose of BrdU injection (Fig. S4C). To further assess the turnover of mTECs, mice were exposed to BrdU water for 1 week to achieve incorporation of BrdU in about 50% mTECs; BrdU water was then withdrawn and retention was measured at various times thereafter. During the chase period, BrdU$^+$ mTECs diminished at a similar rate between wide-type and *Kdm6b*$^{fl/fl}$*Foxn1*-Cre mice (Fig. S4D), suggesting that cell turnover was not influenced by Kdm6b deficiency. Considering the combined effect of slightly less proliferation and more apoptosis in *Kdm6b*$^{fl/fl}$*Foxn1*-Cre mTECs, the similar level of BrdU$^+$ mTECs between wide-type and *Kdm6b*$^{fl/fl}$*Foxn1*-Cre mTECs is reasonable. Thus, increased apoptotic mTECs together with slightly decreased proliferation in *Kdm6b*$^{fl/fl}$*Foxn1*-Cre mTECs account mainly for the reduced number of mTECs, consequently resulting in a shrink mTEC compartment.

The antiapoptotic effect of Kdm6b has been linked to the demethylation of H3K27me3 at the regulatory elements of the antiapoptotic gene *Bcl2* [38]. Consistent with these findings, the mRNA of *Bcl-2*, but not *Bcl-xl* or *Mcl-1*, was downregulated in mTECs of *Kdm6b*$^{fl/fl}$*Foxn1*-Cre mice, comparable (Fig. 5b). Chromatin immunoprecipitation (ChIP)-qPCR further confirmed that the level of H3K27me3 at the promoter and enhancer region of *Bcl2* was dramatically higher in sorted primary mTECs of *Kdm6b*$^{fl/fl}$*Foxn1*-Cre mice (Fig. 5c), suggesting that the reduced expression of Bcl-2 was caused by increased the level of repressive H3K27me3.

Kdm6b facilitates the expression of Aire-dependent TRA genes in mTECs

We previously showed that the mRNA level of TRA genes was reduced in the total CD45$^-$EpCAM$^+$ TEC population of *Kdm6b*$^{fl/fl}$*Foxn1*-Cre thymus (Fig. S3). However, whether the reduction of TRAs was secondary to decreased number of mTECs in *Kdm6b*$^{fl/fl}$*Foxn1*-Cre mice or primarily due to intrinsically impaired capability of mTECs to express TRA genes was unclear. To answer this question, we performed gene expression profiling of MHCII^{hi}CD80^{hi} mature mTECs sorted from 4-week-old *Kdm6b*$^{fl/fl}$*Foxn1*-Cre mice and wild-type controls. Gene expression profiling of these cells revealed that Kdm6b upregulated the expression of over 1800 genes, while it repressed about 1000 different genes (Fig. 6a). Thus, Kdm6b has a very broad and dramatic effect on the global gene expression profile of mTECs. Next, to understand whether and to what extent Kdm6b regulates TRA expression, we compared the overlap of Kdm6b-upregulated genes with tissue-restricted genes (derived from GSE53111) and found that more than 50% of Kdm6b up-regulated genes are TRAs (Fig. 6b). Subsequent RT-qPCR validated our gene expression profile (Fig. 6c).

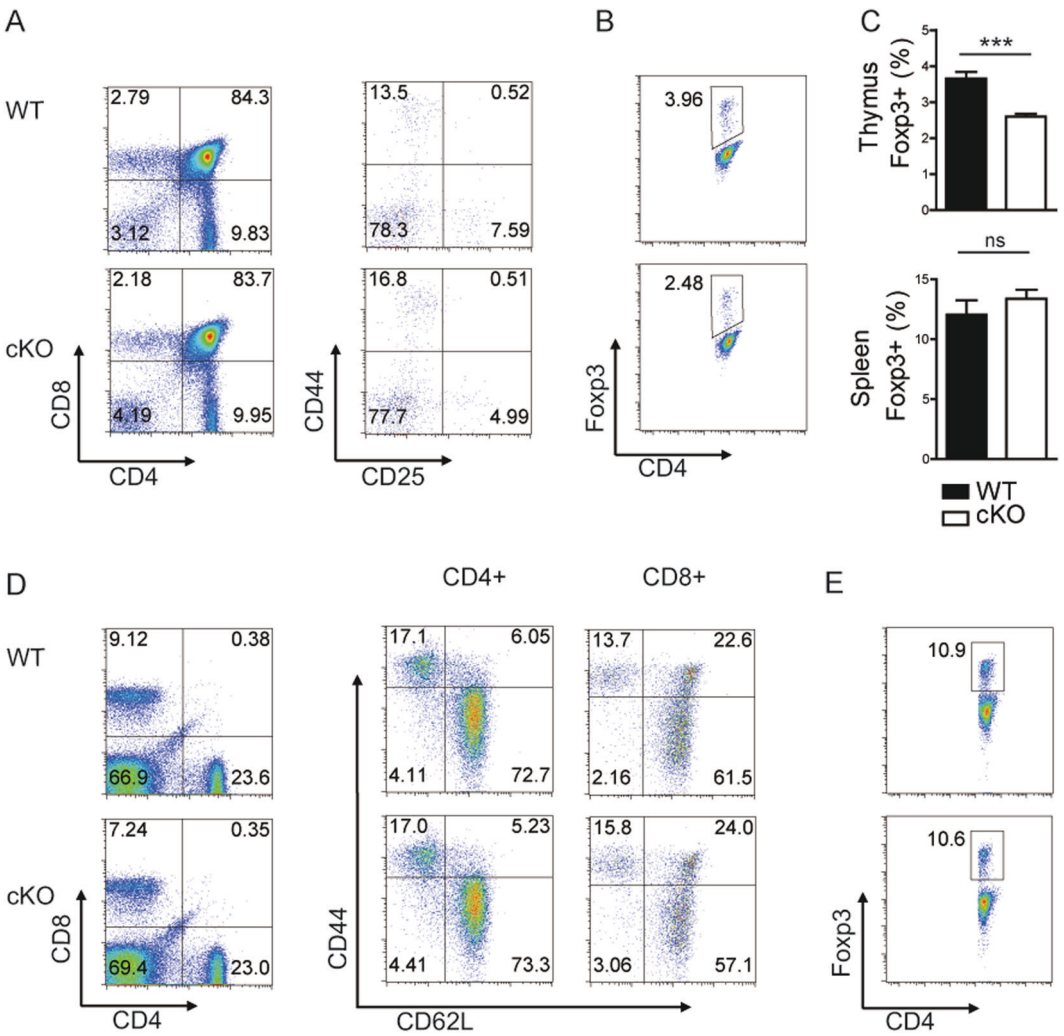

Fig. 3 Impaired differentiation of thymic Treg cells in *Kdm6b*$^{fl/fl}$ *Foxn1*-Cre thymus. a Flow cytometry analysis of CD4, CD8, CD25 and CD44 expression by thymocytes from *Kdm6b*$^{fl/fl}$*Foxn1*-Cre and wild-type mice for the cell surface marker ($n = 6$ per genotype). **b** Flow cytometry analysis of thymic Treg cells from *Kdm6b*$^{fl/fl}$*Foxn1*-Cre and wild-type mice ($n = 6$ per genotype). **c** Percentages of Treg cells in the thymus (top) and spleen (bottom) ($n = 6$ per genotype). **d** Flow cytometry analysis of CD4, CD8, CD44 and CD62L expression by splenocytes from *Kdm6b*$^{fl/fl}$*Foxn1*-Cre and wild-type mice ($n = 6$ per genotype). **e** Flow cytometry analysis of Treg cells in the spleens from *Kdm6b*$^{fl/fl}$*Foxn1*-Cre and wild-type mice ($n = 6$ per genotype).

TRAs are largely regulated by Aire and Fezf2. We reasoned that Kdm6b might regulate the expression level of these two transcriptional factors or cooperate with them to control TRA gene expression. To test these possibilities, we first checked the expression of Aire or Fezf2 in primary mTECs of *Kdm6b*$^{fl/fl}$*Foxn1*-Cre mice and found both of them were similar in FACS-sorted MHCII^{hi}CD80^{hi} mature mTECs (Fig. 6c). RANK, CD40 and LTβR stimulation are known to induce differentiation of mature mTECs expressing Aire and Fezf2. However, we did not observe that these signaling could upregulate Kdm6b mRNA in the in vitro fetal thymus organ culture (FTOC) system (Fig. S5A). Moreover, treatment with GSK-J4, an inhibitor of H3K27 demethylase, in FTOC system did not affect Aire and Fezf2 expression (Fig. S5B). The data suggest that Kdm6b might not be involved in RANK, CD40 and LTβR-mediated mTEC progenitor differentiation.

Next, we examined whether Kdm6b cooperates with Aire and/or Fezf2 to regulate TRA expression. Our bioinformatics analysis showed that Kdm6b-induced genes did not overlap with Fezf2-induced genes, while their association with Aire-induced genes was significantly dramatic (Fig. 6d). To confirm this observation, we further checked the expression of the top 20 Fezf2-dependent genes (derived from GSE69105) in our RNA-seq and found their expression levels were almost identical between Kdm6b-deficient mature mTECs and WT controls (Fig. 6e). Meanwhile, we found that 11 of 20 top Kdm6b-induced genes belong to TRAs, and 10 of these 11 TRA genes were strikingly Aire-dependent, whereas only 1 of them was Fezf2-dependent

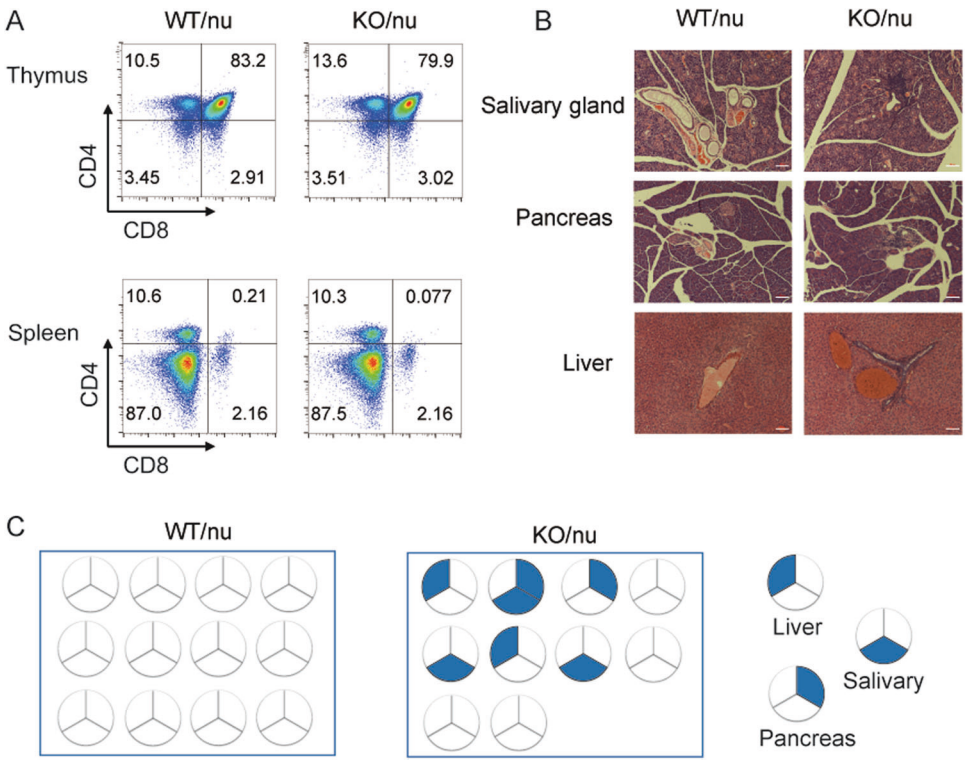

Fig. 4 Kdm6b deficiency leads to autoimmunity. a Flow cytometric profiles of thymocytes for the expression of CD4 and CD8 from 2DG-FTOC thymic lobes grafted under kidney capsules of nude mice for 10 weeks (top). Bottom panels show flow cytometric profiles of splenocytes for the expression of CD4 and CD8 from the nude mice grafted with indicated thymic lobes (wild-type, $n = 12$; *Kdm6b*$^{-/-}$, $n = 10$). **b** Representative images of H&E staining of tissue sections of the salivary gland, pancreas, and liver from nude mice transferred with *Kdm6b*$^{-/-}$ and wild-type thymi. Scale bars, 100 μm (wild-type, $n = 12$; *Kdm6b*$^{-/-}$, $n = 10$). **c** Summary of lymphocyte infiltrates in the nude mice transplanted with wide-type and *Kdm6b*$^{-/-}$ thymi. Each circle represents an individual mouse, with corresponding organ indicated by the key on the right.

(Fig. 6f). Therefore, Kdm6b mainly regulated Aire-dependent TRA gene expression.

Aire, with its partners, regulates TRA expression through a large functional complex. We speculated that Kdm6b might regulate the expression of TRA genes by interacting with Aire. To test this hypothesis, we performed co-immunoprecipitation (Co-IP) experiments with wild-type primary mTECs or HEK293T cells overexpressed with Kdm6b and Aire. However, we did not observe that Kdm6b interacted with Aire in either HEK293T cells or primary mTECs (Fig. S5C and data not shown), suggesting that the interaction between Aire and Kdm6b might be weak and dynamic, or Kdm6b might function separately to regulate Aire-dependent TRA expression.

Kdm6b-dependent TRA genes are associated with a repressive chromatin state

To further dissect the difference among Kdm6b-dependent, Aire-dependent and Fezf2-dependent TRAs, we examined the epigenetic state of primary wild-type mTECs by genome-wide chromatin immunoprecipitation followed by deep sequencing (ChIP-seq) for the bivalent chromatin markers of H3K4me3 and H3K27me3. By cross-referencing with RNA-seq data from ourselves (GSE110505) and the GEO database (GSE53111 for Aire-dependent genes and GSE69105 for Fezf2-dependent genes), we were able to compare the difference of epigenetic states of Kdm6b-dependent, Aire-dependent and Fezf2-dependent TRAs. Not surprisingly, we observed a broadly higher enrichment of H3K27me3 in the vicinity of TSS and gene-bodies of downregulated genes compared to the genes upregulated after Kdm6b deletion while the H3K4me3 level was comparable around TSS between Kdm6b-upregulated genes and Kdm6b downregulated genes (Fig. 7a). These data indicate Kdm6b-dependent genes possessed a repressive chromatin state and Kdm6b-dependent H3K27 demethylation was critically involved in the regulation of their expression. Consistent with previous studies that show genes regulated by Aire have a repressive chromatin state, we found that genes downregulated in Aire-deficient mTECs were characterized by higher abundance of H3K27me3 and lower abundance of H3K4me3 compared to Aire-upregulated genes (Fig. 7b), further confirming the epigenetic landscape of Kdm6b-dependent genes observed here was reliable. We further analyzed the epigenetic landscape of Fezf2-dependent genes. However, there was no notable difference of H3K4me3 and H3K27me3 abundance between Fezf2-upregulated and Fezf2-downregulated genes after Fezf2 deletion (Fig. 7c). These data suggest that Kdm6b-dependent TRAs have a repressive chromatin state, similar to Aire-dependent TRAs, but different from Fezf2-dependent TRAs.

Due to the dramatically reduced cell number of mTECs, we were not able to perform ChIP-seq in *Kdm6b*$^{fl/fl}$*Foxn1*-Cre mTECs. Alternatively, we employed ChIP-qPCR method to analyze the distribution of H3K27me3 across the promoter regions of Kdm6b-dependent TRA genes in wild-type and *Kdm6b*$^{fl/fl}$*Foxn1*-Cre mTECs. Our ChIP assay

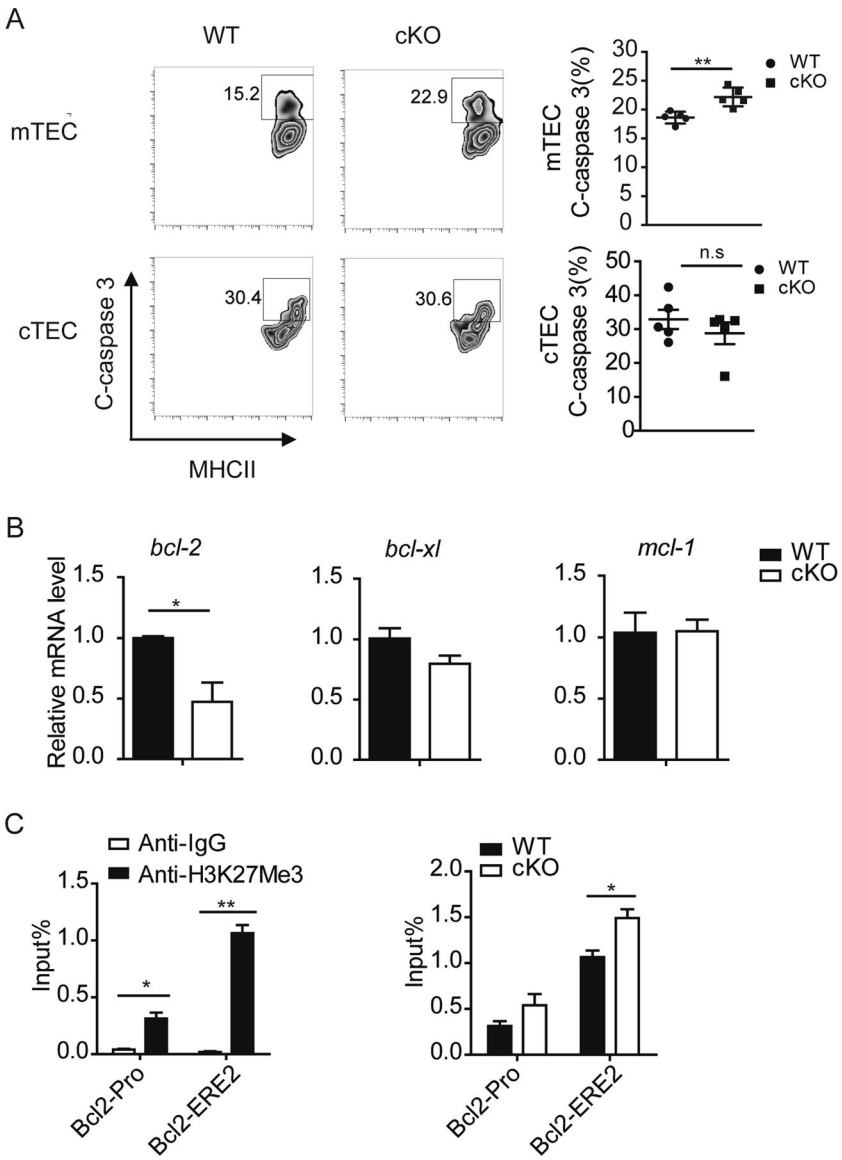

Fig. 5 Kdm6b promotes cell survival of mTECs. a Flow cytometric profiles of cTECs (gated on $CD45^{-}EpCAM^{+}Ly51^{+}UEA^{-}$) and mTECs (gated on $CD45^{-}EpCAM^{+}Ly51^{-}UEA^{+}$) for the expression of C-caspase 3, an apoptotic marker(left). Frequencies of apoptotic mTECs and cTECs are shown on the right ($n = 5$ per genotype). **b** Expression of *Bcl2*, *Bcl-xl* and *Mcl-1* in mTECs from 4-week-old wild-type and $Kdm6b^{fl/fl}$ *Foxn1*-Cre mice ($n = 5$ per genotype). **c** The enrichment of H3K27me3 at the enhancer and promoter region of *Bcl-2* in wild-type and $Kdm6b^{fl/fl}$*Foxn1*-Cre mTECs (representative result from two independent experiments).

showed that H3K27me3 was significantly enriched at the promoter regions of Kdm6b-dependent TRAs in wild-type mTECs compared with IgG (Fig. 7d). Furthermore, there was significantly increased enrichment of H3K27me3 at the promoter regions of Kdm6b-dependent TRAs-*Cxcl3*, *Mefv*, *Dcstamp*, *Kcnd3* in $Kdm6b^{fl/fl}$*Foxn1*-Cre mTECs (Fig. 7e), indicating that the reduced expression of Kdm6b-dependent TRAs in $Kdm6b^{fl/fl}$*Foxn1*-Cre mTECs was largely due to the increased level of repressive H3K27me3 at their promoter regions caused by Kdm6b deletion.

Discussion

We have here identified the H3K27 demethylase Kdm6b as a vital regulator of both homeostatic survival and TRA expression in mTECs. Deficiency of Kdm6b in TEC populations dramatically reduced the medullary compartment to almost one-third of wild-type controls due to its anti-apoptotic function. On the other hand, Kdm6b did not play an essential role in the maturation of mTECs, as in its absence the ratio of immature mTECs to mature mTECs was maintained normally. Moreover, Kdm6b regulated the expression of a great number of Aire-dependent TRA genes. Collectively, the loss of mTECs combined with incapability of proper expression of TRAs in Kdm6b-deficient thymus resulted in the impaired mTEC-mediated negative selection, thymic Treg cell generation and subsequent multi-organ autoimmune diseases. Taken together, these data demonstrated an important role of Kdm6b in the postnatal regulation of mTEC cellularity and function.

Kdm6b seems not to be critical for mTEC development and TRA expression at embryonic stage. It might be due to the low expression of Kdm6b during embryonic stage since

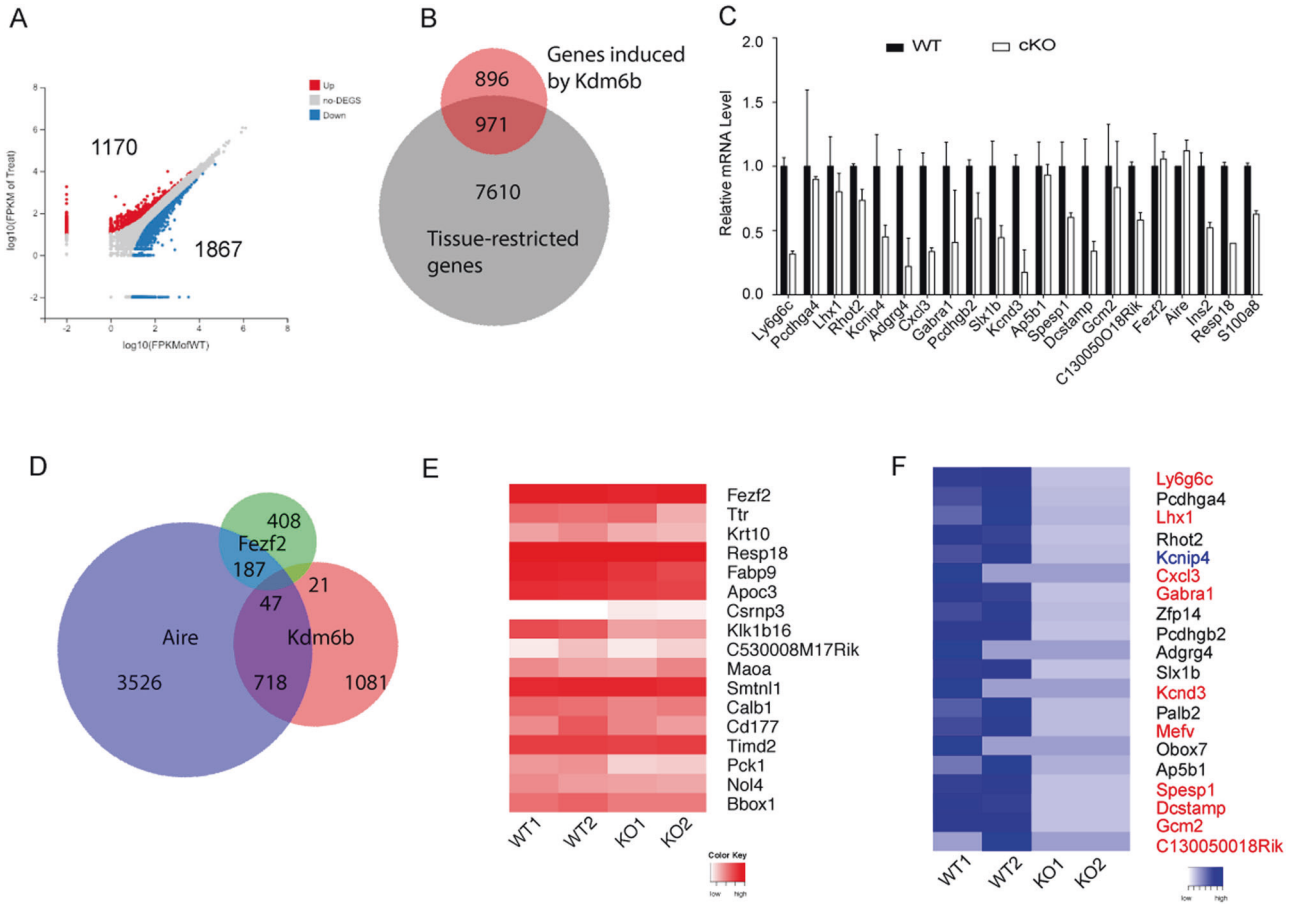

Fig. 6 Kdm6b regulates a considerable fraction of Aire-dependent TRAs. a A scatterplot of RNA-seq comparing gene expression values in Kdm6b-deficient $CD80^{hi}MHC^{hi}$ mature mTECs and wide-type controls. **b** A comparison of Kdm6b-induced genes and whole TRA genes. **c** qPCR analysis of Kdm6b-dependent TRAs, *Fezf2*, *Aire* and Aire-dependent TRAs in $Kdm6b^{fl/fl}$*Foxn1*-Cre mTECs ($n = 2$ per genotype). **d** A Venn diagram of the Kdm6b-dependent, Aire-dependent and Fezf2-dependent genes. Most of Kdm6b-dependent genes are different from Fezf2-dependent genes (GSE69105), but strongly overlapped with Aire-dependent genes (GSE53111) collected from the database (fold change > 1.5, $p < 0.05$). **e** The expression of *Fezf2* and top 20 Fezf2-dependent genes in $Kdm6b^{fl/fl}$*Foxn1*-Cre mature mTECs. **f** The top 20 of Kdm6b-dependent genes. Red colors are Aire-dependent TRA genes ($n = 10$), while blue color is Fezf2-dependent TRA gene.

its mRNA was gradually increased postnatally. To our surprise, Kdm6b expression is not induced in FTOC by RANK, CD40 or LTβR-activated signaling, the most well-known signaling that promotes mTEC differentiation (Fig. S5). Although we currently do not know which signals upregulate Kdm6b expression in TECs, our data revealed the critical function of Kdm6b in mTEC homeostasis, especially after birth when Kdm6b expression is at a high level.

For the dramatic loss of mTECs in Kdm6b-deficient mice, we found that Kdm6b only limited the pool of apoptotic mTECs although Kdm6b was comparably expressed in cTECs. Besides its anti-apoptotic action, Kdm6b could induce or inhibit proliferation in different cell types; however, we only observed slightly reduced proliferation of mTECs but not significantly in the absence of Kdm6b, which implied that reduced cell proliferation is a minor contributor to the observed defect in the mTEC compartment. Lastly, beyond the important role of Kdm6b in the maintenance of mTEC survival, we cannot rule out the possibility that Kdm6b might also affect mTEC progenitor differentiation into $mTEC^{low}$ populations in vivo. Although our in vitro FTOC experiment by adding RANKL, anti-CD40, anti-LTβR did not induce Kdm6b expression, and under this condition, GSK-J4 neither caused a reduction in Aire or Fezf2 expression suggesting that H3K27me3 might not be involved in mTEC progenitor differentiation in vitro, there still exists the possibility that Kdm6b somehow could regulate mTEC progenitor differentiation in vivo, which needs to be further investigated.

The autoimmunity in $Kdm6b^{fl/fl}$*Foxn1*-Cre mice is milder than the autoimmune phenotype in Aire-KO and Fezf2-KO mice. This might be due to that Kdm6b only regulates a fraction of Aire-dependent TRA genes. On the other hand, Kdm6b-dependent defects might partially be compensated

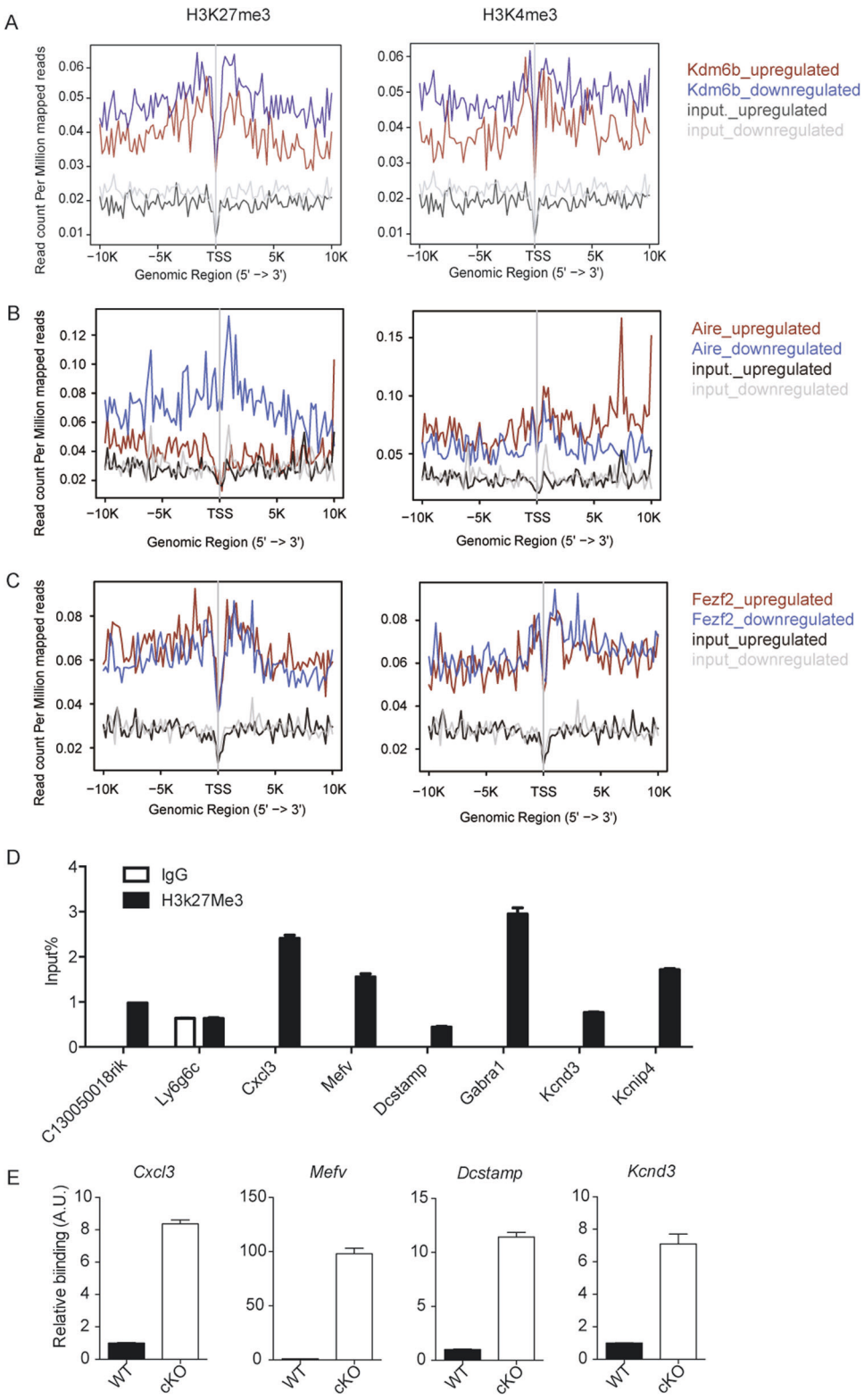

Fig. 7 Kdm6b deficiency results in the increased enrichment of repressive H3K27me3 at the promoter regions of Kdm6b-regulated TRA genes. Genome-wide distribution of average H3K27me3 and H3K4me3 ChIP signals across genes downregulated and upregulated by Kdm6b deletion (**a**), Aire deletion (**b**) and Fezf2 deletion (**c**) with cross-referencing with RNA data from ourselves and GEO database. **d** ChIP-qPCR analysis of H3K27me3 enrichment at the promoter regions of Kdm6b-dependent TRAs, compared to IgG (representative result from two independent experiments). **e** ChIP-qPCR analysis to compare the enrichment of H3K27me3 at the promoter regions of Kdm6b-dependent TRAs between wild-type and *Kdm6b*$^{fl/fl}$*Foxn1*-Cre mTECs (representative result from two independent experiments).

by the other H3K27 demethylase Kdm6a. Further study is required to investigate the impact of H3K27 methylation on the development, maintenance and function of mTECs by using the double knock-out mice of Kdm6b and Kdm6a.

Promiscuous gene expression of TRAs is essential for mTEC-mediated negative selection of self-reactive T cells. To date, Aire and Fezf2 are the only two regulators to directly regulate TRA expression [7]. Here, we found that

Kdm6b regulated a sizable proportion of Aire-dependent TRA expression. Since Aire-dependent TRAs are characteristic of enrichment of H3K27me3 and H3K4me0, it was convincible that Aire coopts Kdm6b to remove the repressive H3K27me3 and promote Aire-dependent TRA expression. However, we did not observe Kdm6b control the expression of Aire, or co-localize with Aire in primary mTECs or HEK293T cells (Fig. 5b). This might be due to that the interaction between Kdm6b and Aire is weak and highly dynamic, or Kdm6b changes the chromatin accessibility before Aire binding and prepares them for Aire induction. For Fezf2-dependent TRAs, although our data showed there was no global difference between Fezf2-upregulated genes and Fezf2-downregulated genes in terms of H3K4me3 and H3K27me3, we cannot exclude the possibility that epigenetic mechanisms were involved in the regulation of Fezf2-dependent TRA expression.

In summary, our study provides mechanistic insights into the impact of Kdm6b in the postnatal maintenance of mTECs, as well as on the regulation of TRA genes, especially Aire-dependent TRA genes, which highlights the dual role of Kdm6b-mediated H3K27 demethylation in mTEC-mediated immunological tolerance.

Materials and methods

Mice

Kdm6b$^{fl/fl}$ mice and *Kdm6b*$^{-/-}$ mice of C57BL/6 background have been described previously [29]. *Foxn1*-cre mice on the same background were kindly provided by Dr T. Boehm. BALB/c nude mice were purchased from the Shanghai Laboratory Animal Center, Chinese Academy of Sciences (Shanghai, China). All mice were maintained under specific pathogen-free conditions. Animal experiments were handled in accordance with the guide for the care and use of laboratory animals and were approved by the institutional biomedical research ethics committee of the Shanghai Institutes for Biological Sciences, Chinese Academy of Sciences.

Antibodies

The following antibodies were used: Alexa-Fluor® 700 anti-mouse CD4 (eBioscience, GK1.5), PE-Cy7 anti-mouse CD8α (BD, 53–6.7), PE anti-mouse CD25 (BD, PC61), APC anti-mouse CD44 (BD, IM7), FITC anti-mouse CD62L (Biolegend, MEL-14), PE-Cy7 anti-mouse CD45 (Biolegend, 30-F11), PE anti-mouse EpCAM (Biolegend, G8.8), FITC anti-mouse UEA1 (Sigma, L9006), Alexa-Fluor® 647 anti-mouse Ly51 (Biolegend, 6C3), V500 anti-mouse MHCII (BD, M5/114.15.2), APC anti-mouse CD80 (eBioscience, 16–10A1), eFluor 450 anti-mouse Ki67 (eBioscience, SolA15), Cleaved Caspase-3 (Cell Signaling Technology, #9661), Alexa-Fluor® 647 anti-mouse Aire (eBioscience, 5H12),PE anti-mouse Foxp3(BD, MF23), Alexa Flour® 488 anti-rabbit IgG (Invitrogen, A-11034), Normal rabbit IgG (Santa Cruz, sc-2027), anti-H3K27me3 (Millipore, #07–449), anti-mouse CD16/32 (Biolegend, 93).

Flow cytometry and cell sorting

Mouse thymic epithelial cells were isolated as described previously [39]. Briefly, the harvested thymi were minced and digested in RPMI1640 medium containing Liberase TH (Roche) and DNase I (Roche), then cells were stained for flow cytometry analysis or separated using a three-layer Percoll gradient (GE Healthcare) with specific gravities of 1.115, 1.065, and 1.0. Enriched epithelial cells were used for cell sorting. mTECs and cTECs were gated as CD45$^-$EpCAM$^+$UEA$^+$Ly51$^-$ and CD45$^-$EpCAM$^+$UEA$^-$Ly51$^+$, respectively. The expression of MHCII and CD80 on mTECs and cTECs were further analyzed. Aire$^+$ positive mTECs were detected using Foxp3/Transcription Factor Staining Buffer Set (eBioscience, 00–5523). Apoptosis and proliferation of mTECs were represented by the percentage of Cleaved Caspase-3 and Ki67 positive cells stained with BD Cytofix/Cytoperm™ Plus Fixation/Permeabilization Kit (BD, 554715). Treg cells in the thymus and spleen were defined as CD4$^+$CD25$^+$Foxp3$^+$. The CD4$^+$/CD8$^+$single positive, CD4$^+$CD8$^+$double positive and CD4$^-$CD8$^-$double negative (DN1-DN4) T cells in the thymi were also analyzed with indicated antibodies. Flow cytometric analysis was performed with Gallios Flow Cytometer (Beckman Coulter) or FlowJo software (Tree Star Inc).

BrdU administration

BrdU was administered as previously described [34]. Mice were intraperitoneally injected with 1.5 mg BrdU (Sigma Aldrich) in PBS for a single pulse labeling. BrdU positive mTECs were analyzed by flow cytometry 24 h after BrdU labeling. Continuous labeling was maintained by incorporation of 0.8 mg/ml BrdU in sterile drinking water with artificial sweetener for 7 days. BrdU positive mTECs were analyzed by flow cytometry at day 0, 7 and 14 after BrdU labeling.

FTOCs and thymic transplantation

Thymic lobes were isolated from embryos at E14.5 of gestation and cultured for 4 days on Nucleopore filters (Millipore, ATTP14250) submerged in RPMI1640 medium, supplemented with 10% fetal bovine serum (FBS) (Gibco), 100 U/ml penicillin (Gibco), 100 μg/ml streptomycin (Gibco), 2mM L-glutamate (Gibco), 50 μM 2-mercaptoethanol (Sigma

Aldrich) and 1.35 mM 2'-deoxyguanosine (2-DG) (Sigma Aldrich, D0901). 2-DG treated FTOCs of *Kdm6b*$^{+/+}$ or *Kdm6b*$^{-/-}$ mice were washed in PBS and transplanted under the kidney capsules of 8-week-old female nude mice (BALB/c background). T cells reconstitution in the transplanted mice were confirmed by flow cytometry 10 weeks later. Organs of transplanted mice were harvested and subjected to flow cytometry and histology analysis.

Histology and immunofluorescence

For histology analysis, tissues were fixed in 4% paraformaldehyde, embedded in paraffin blocks and cut into 5 μm thick sections. Sections were stained with hematoxylin and eosin, and photographed with a general optical microscope with a camera (Carl Zeiss). For immunofluorescence analysis, thymi from mice of different age were embedded in OCT compound and frozen in −80°C refrigerator. Cryostat sections were cut and stained with K5, K8, UEA1, Aire, ERTR7 and MTS10. Images were collected using a Zeiss laser-scanning confocal microscope (LSM Meta 510).

ChIP

ChIP assays were performed with EZ-ChIP™ Chromatin Immunoprecipitation Kit (Millipore, #17–371). For ChIP-seq analysis, rabbit anti-H3K27me3 and anti-H3K4me3 were used for immunoprecipitation. About 5×10^5 sorted mTECs of wild-type and 2 μg antibodies were used for each immunoprecipitation. ChIPed DNA was amplified by SeqPlex™ Enhanced DNA Amplification Kit (Sigma Aldrich, SEQXE) according to manufacturer's protocol and sequenced. For ChIP-qPCR analysis, 2×10^5 pooled mTECs from *Kdm6b*$^{fl/fl}$ or *Kdm6b*$^{fl/fl}$*Foxn1*-cre mice were sorted by flow cytometry and immunoprecipitated with rabbit anti-H3K27me3 and normal rabbit IgG. ChIPed DNA was amplified as above and used for real-time PCR analysis.

RNA-seq analysis

Mature mTECs from three pairs of *Kdm6b*$^{fl/fl}$ and *Kdm6b*$^{fl/fl}$ Foxn1-cre mice were sorted by flow cytometry. Total RNA was isolated with a RNeasy Mini Kit (QIAGEN, 74104). cDNA was amplified by REPLI-g WTA Single Cell Kit (QIAGEN, 150063) following the manufacturer's instructions and sequenced. The raw data were mapped to a reference genome (mm10) using Bowtie. Levels of gene expression were quantified using the RSEM software package. Differentially expressed genes were obtained by setting a false discovery rate (FDR) threshold of 0.001 and fold changes cut off at 1.5. Selected genes were verified by real time PCR.

Real time quantitative PCR

Total RNA was extracted from 2-DG treated FTOCs or TECs sorted by FACS using a RNeasy Mini Kit (QIAGEN, 74104) or TRIzol® Reagent (Invitrogen, 15596–018) following the manufacturer's instructions. cDNA was reversely transcribed with a PrimeScript™ RT Master Mix (TakaRa, RR036A). Quantitative PCR of target genes was performed using SYBR Green Gene Expression PCR Master Mix (TakaRa, RR420A). For RT-qPCR analysis, expression of target genes was normalized by *GAPDH* expression using the $2^{-\Delta\Delta Ct}$ methods. For ChIP-qPCR analysis, input% of target genomic region was calculated.

Statistical analysis

Results are representative of more than two independent experiments. Unless indicated otherwise, data are shown as the mean ± SEM. The significance of all paired data was determined using the two-tailed Student's *t* test ($*p < 0.05$; $**p < 0.01$; $***p < 0.001$; NS, not significant).

Accession numbers

The GEO accession number for the high-throughput sequencing reported in this paper is GSE110505

Acknowledgements We thank Dr T. Boehm for the *Foxn1*-Cre transgenic mouse, Drs H. Wei, Y. Liu and B. Fu for their suggestions, B. Peng, B. Qian and Q. Jing for their support. This study was supported by grants from the National Program on Key Research (2018YFA0107500, 2016YFC1302400), the National Natural Science Foundation of China (91949102, 91742113, 31570902, 81771752 and 31370881) and the Guangzhou Key Medical Discipline Construction Project Fund.

Compliance with ethical standards

Conflict of interest The authors declare that they have no conflict of interest.

References

1. Rodewald HR. Thymus organogenesis. Annu Rev Immunol. 2008;26:355–88.
2. Anderson G, Takahama Y. Thymic epithelial cells: working class heroes for T cell development and repertoire selection. Trends Immunol. 2012;33:256–63.
3. Aschenbrenner K, D'Cruz LM, Vollmann EH, Hinterberger M, Emmerich J, Swee LK, et al. Selection of Foxp3+ regulatory T cells specific for self antigen expressed and presented by Aire+ medullary thymic epithelial cells. Nat Immunol. 2007;8:351–8.
4. Cowan JE, Parnell SM, Nakamura K, Caamano JH, Lane PJ, Jenkinson EJ, et al. The thymic medulla is required for Foxp3+

regulatory but not conventional CD4+ thymocyte development. J Exp Med. 2013;210:675–81.
5. Derbinski J, Schulte A, Kyewski B, Klein L. Promiscuous gene expression in medullary thymic epithelial cells mirrors the peripheral self. Nat Immunol. 2001;2:1032–9.
6. Klein L, Hinterberger M, Wirnsberger G, Kyewski B. Antigen presentation in the thymus for positive selection and central tolerance induction. Nat Rev Immunol. 2009;9:833–44.
7. Takaba H, Morishita Y, Tomofuji Y, Danks L, Nitta T, Komatsu N, et al. Fezf2 orchestrates a thymic program of self-antigen expression for immune tolerance. Cell. 2015;163:975–87.
8. Anderson MS, Venanzi ES, Klein L, Chen Z, Berzins SP, Turley SJ, et al. Projection of an immunological self shadow within the thymus by the aire protein. Science. 2002;298:1395–401.
9. Nagamine K, Peterson P, Scott HS, Kudoh J, Minoshima S, Heino M, et al. Positional cloning of the APECED gene. Nat Genet. 1997;17:393–8.
10. Rossi SW, Jenkinson WE, Anderson G, Jenkinson EJ. Clonal analysis reveals a common progenitor for thymic cortical and medullary epithelium. Nature. 2006;441:988–91.
11. Akiyama T, Shimo Y, Yanai H, Qin J, Ohshima D, Maruyama Y, et al. The tumor necrosis factor family receptors RANK and CD40 cooperatively establish the thymic medullary microenvironment and self-tolerance. Immunity. 2008;29:423–37.
12. Hikosaka Y, Nitta T, Ohigashi I, Yano K, Ishimaru N, Hayashi Y, et al. The cytokine RANKL produced by positively selected thymocytes fosters medullary thymic epithelial cells that express autoimmune regulator. Immunity. 2008;29:438–50.
13. Rossi SW, Kim MY, Leibbrandt A, Parnell SM, Jenkinson WE, Glanville SH, et al. RANK signals from CD4(+)3(−) inducer cells regulate development of Aire-expressing epithelial cells in the thymic medulla. J Exp Med. 2007;204:1267–72.
14. Akiyama T, Maeda S, Yamane S, Ogino K, Kasai M, Kajiura F, et al. Dependence of self-tolerance on TRAF6-directed development of thymic stroma. Science. 2005;308:248–51.
15. Kajiura F, Sun S, Nomura T, Izumi K, Ueno T, Bando Y, et al. NF-kappa B-inducing kinase establishes self-tolerance in a thymic stroma-dependent manner. J Immunol. 2004;172:2067–75.
16. Burkly L, Hession C, Ogata L, Reilly C, Marconi LA, Olson D, et al. Expression of relB is required for the development of thymic medulla and dendritic cells. Nature. 1995;373:531–6.
17. Zhang X, Wang H, Claudio E, Brown K, Siebenlist U. A role for the IkappaB family member Bcl-3 in the control of central immunologic tolerance. Immunity. 2007;27:438–52.
18. Takahama Y, Ohigashi I, Baik S, Anderson G. Generation of diversity in thymic epithelial cells. Nat Rev Immunol. 2017;17:295–305.
19. Atlasi Y, Stunnenberg HG. The interplay of epigenetic marks during stem cell differentiation and development. Nat Rev Genet. 2017;18:643–58.
20. Chuprin A, Avin A, Goldfarb Y, Herzig Y, Levi B, Jacob A, et al. The deacetylase Sirt1 is an essential regulator of Aire-mediated induction of central immunological tolerance. Nat Immunol. 2015;16:737–45.
21. Waterfield M, Khan IS, Cortez JT, Fan U, Metzger T, Greer A, et al. The transcriptional regulator Aire coopts the repressive ATF7ip-MBD1 complex for the induction of immunotolerance. Nat Immunol. 2014;15:258–65.
22. Koh AS, Kuo AJ, Park SY, Cheung P, Abramson J, Bua D, et al. Aire employs a histone-binding module to mediate immunological tolerance, linking chromatin regulation with organ-specific autoimmunity. Proc Natl Acad Sci USA. 2008;105:15878–83.
23. Koh AS, Miller EL, Buenrostro JD, Moskowitz DM, Wang J, Greenleaf WJ, et al. Rapid chromatin repression by Aire provides precise control of immune tolerance. Nat Immunol. 2018;19:162–72.
24. Sansom SN, Shikama-Dorn N, Zhanybekova S, Nusspaumer G, Macaulay IC, Deadman ME, et al. Population and single-cell genomics reveal the Aire dependency, relief from Polycomb silencing, and distribution of self-antigen expression in thymic epithelia. Genome Res. 2014;24:1918–31.
25. Swigut T, Wysocka J. H3K27 demethylases, at long last. Cell. 2007;131:29–32.
26. Satoh T, Takeuchi O, Vandenbon A, Yasuda K, Tanaka Y, Kumagai Y, et al. The Jmjd3-Irf4 axis regulates M2 macrophage polarization and host responses against helminth infection. Nat Immunol. 2010;11:936–44.
27. Manna S, Kim JK, Bauge C, Cam M, Zhao Y, Shetty J, et al. Histone H3 Lysine 27 demethylases Jmjd3 and Utx are required for T-cell differentiation. Nat Commun. 2015;6:8152.
28. Northrup D, Yagi R, Cui K, Proctor WR, Wang C, Placek K, et al. Histone demethylases UTX and JMJD3 are required for NKT cell development in mice. Cell Biosci. 2017;7:25.
29. Liu Z, Cao W, Xu L, Chen X, Zhan Y, Yang Q, et al. The histone H3 lysine-27 demethylase Jmjd3 plays a critical role in specific regulation of Th17 cell differentiation. J Mol Cell Biol. 2015;7:505–16.
30. Ciofani M, Madar A, Galan C, Sellars M, Mace K, Pauli F, et al. A validated regulatory network for Th17 cell specification. Cell. 2012;151:289–303.
31. Burgold T, Voituron N, Caganova M, Tripathi PP, Menuet C, Tusi BK, et al. The H3K27 demethylase JMJD3 is required for maintenance of the embryonic respiratory neuronal network, neonatal breathing, and survival. Cell Rep. 2012;2:1244–58.
32. Zhang F, Xu L, Xu L, Xu Q, Li D, Yang Y, et al. JMJD3 promotes chondrocyte proliferation and hypertrophy during endochondral bone formation in mice. J Mol Cell Biol. 2015;7:23–34.
33. Gray DH, Seach N, Ueno T, Milton MK, Liston A, Lew AM, et al. Developmental kinetics, turnover, and stimulatory capacity of thymic epithelial cells. Blood. 2006;108:3777–85.
34. Gray D, Abramson J, Benoist C, Mathis D. Proliferative arrest and rapid turnover of thymic epithelial cells expressing Aire. J Exp Med. 2007;204:2521–8.
35. Takahama Y. Journey through the thymus: stromal guides for T-cell development and selection. Nat Rev Immunol. 2006;6:127–35.
36. Jiang W, Anderson MS, Bronson R, Mathis D, Benoist C. Modifier loci condition autoimmunity provoked by Aire deficiency. J Exp Med. 2005;202:805–15.
37. Barradas M, Anderton E, Acosta JC, Li S, Banito A, Rodriguez-Niedenfuhr M, et al. Histone demethylase JMJD3 contributes to epigenetic control of INK4a/ARF by oncogenic RAS. Genes Dev. 2009;23:1177–82.
38. Svotelis A, Bianco S, Madore J, Huppe G, Nordell-Markovits A, Mes-Masson AM, et al. H3K27 demethylation by JMJD3 at a poised enhancer of anti-apoptotic gene BCL2 determines ERalpha ligand dependency. EMBO J. 2011;30:3947–61.
39. Xing Y, Hogquist KA. Isolation, identification, and purification of murine thymic epithelial cells. J Vis Exp. 2014;8:e51780.